ASTRONOMY
AND
ASTROPHYSICS

Submillimetre polarization and constraints on dust grain alignment

J.S. Greaves[1], W.S. Holland[1], N.R. Minchin[2], A.G. Murray[2,3], and J.A. Stevens[1,4]

[1] Joint Astronomy Centre, 660 N. A'ohōkū Place, University Park, Hilo, HI 96720, USA
[2] Department of Physics, Queen Mary and Westfield College, Mile End Road, London E1 4NS, UK
[3] Moray College, Moray Street, Elgin IV30 1JJ, UK
[4] Mullard Space Science Laboratory, University College London, Holmbury St. Mary, Dorking, Surrey RH5 6NT, UK

Abstract. Polarization at 800 and 1100 μm has been observed in the star-forming regions Mon R2, DR21 and W3-IRS4. These data have been used to test proposed mechanisms for producing polarized dust emission in the submillimetre. It was found that illumination effects are not sufficient to explain the observed polarization, and that some degree of grain alignment is required. In general, mechanical alignment (via collisions with molecules) and radiative alignment of asymmetrical grains are the most probable mechanisms.

The degrees and directions of polarization observed in DR21 are found to be wavelength dependent at 800 to 1100 μm. A search of previous JCMT polarimetry results shows that for about half the sources observed, p(1100) is greater than p(800), while in most of the other sources the two values of p are in agreement. A possible explanation for this result is that there are two (or more) non-cospatial grain populations along the line of sight, with different degrees of polarizability and different opacity indices. This can produce bias effects in the polarization percentage and position angle. Thus the choice of wavelength is *not* immaterial in dust emission polarimetry, as is commonly believed.

Key words: ISM: magnetic fields – polarization

1. Introduction

Polarized continuum emission from dust grains has been detected in a wide variety of Galactic sources. It is widely believed that the local magnetic field acts to align elongated grains, so that they spin with their long axes perpendicular to the field. This results in linear polarization, which can be used to measure the direction of the field component in the plane of the sky. The polarization position angle, θ, is perpendicular to the net field within the area observed. The percentage polarization p is not so generally useful, as it is a function of several parameters, including grain alignment efficiency, optical depth, inclination of the field to the plane of the sky, and the amount of local disorder in the field. However, the value of p sometimes correlates with other source properties (e.g. in protostars, Greaves et al. 1997),

Send offprint requests to: J.S. Greaves

and has also been used to constrain grain alignment efficiencies (Roberge 1996, Hildebrand & Dragovan 1997).

Although many data have been obtained on the polarization of dust emission, it is still unclear exactly how the grains are aligned (Hildebrand 1996). Paramagnetic relaxation (Davis & Greenstein 1951) was favoured, but it is now known that this mechanism aligns small grains most efficiently, the opposite to what is observed (e.g. Lazarian 1996a), and that unrealistically large gas and dust temperatures differences are required for molecular clouds (Roberge 1996). Alternatives include superparamagnetism (paramagnetism enhanced by iron compound inclusions in the grains, e.g. Sorrell 1994); mechanical alignment by collisions with gas molecules (Roberge et al. 1995); and radiative alignment where a torque is induced on asymmetrical grains (Draine & Weingartner 1996, 1997). A necessary condition for many of the alignment models is that the grains spin at suprathermal speeds. This spin-up could be due to radiative torque (Draine & Weingartner 1996), or initiated by cosmic rays which release H_2 molecules from grain mantles providing a 'rocket effect' (Sorrell 1995a). Finally, it has been suggested by Onaka (1995) that polarization can arise *without* alignment, if grain heating depends on the cross-section presented to an illuminating source. This mechanism can also affect the polarization if the grains are aligned (Onaka 1996).

We have made polarization observations at 800 and 1100 μm of three star-forming molecular clouds, including Mon R2, W3 and DR21. The results are discussed here, and used to constrain the above models for the production of submillimetre polarization in dust clouds.

2. Observations

The observations were made at the James Clerk Maxwell Telescope (JCMT) in September 1995. The Aberdeen/QMW polarimeter, consisting of a rotating half-waveplate and fixed wire-grid analyser, (Murray 1991, Murray et al. 1992) was used in conjunction with the continuum bolometer instrument UKT14 (Duncan et al. 1990). The observations were made at wavelengths of 800 and 1100 μm.

The observing procedure has been described by Greaves et al. (1994); briefly, photometry was done at 16 equally spaced waveplate positions in a 360° degree cycle, and the sinusoidal

Table 1. Polarization percentages and position angles at 800 and 1100 μm. The values of p and the errors in θ have been corrected for bias due to the positive nature of p (Wardle & Kronberg 1974). Position offsets are in arcseconds; beam sizes were set to 19″ by the use of an aperture, apart from the W3 data, where a diffraction-limited 14″ beam was used.

source	p(800) (%)	θ(800) (°)	p(1100) (%)	θ(1100) (°)
Mon R2				
IRS2	1.90 ± 0.83	90 ± 13	0.72 ± 0.88	83 ± 36
IRS3	1.83 ± 0.36	134 ± 6	2.22 ± 0.76	160 ± 10
DR21				
(0,0)	2.34 ± 0.27	20 ± 3	1.39 ± 0.21	14 ± 4
(0,−14)	1.50 ± 0.21	30 ± 4	3.47 ± 0.69	16 ± 6
(0,+14)	2.31 ± 0.39	31 ± 5	3.00 ± 0.43	4 ± 4
W3 IRS4				
(0,0)	0.45 ± 0.32	103 ± 22		
(0,+13.5)	2.28 ± 1.06	95 ± 14		
(0,−13.5)	1.15 ± 0.44	29 ± 11		
(+13.5,0)	1.67 ± 0.80	115 ± 14		
(−13.5,0)	3.35 ± 0.91	112 ± 8		

Table 2. Physical properties of the cloud cores, from dust emission maps (Henning et al. 1992; Richardson et al. 1986; Oldham et al. 1994). The dust temperature and gas density are given by T and n(H$_2$). For DR21, the second set of results uses an unpublished JCMT map at 850 μm, with the methods of Richardson et al. (1986) but a 15″ beam instead of 40″; the luminosity is from Harvey et al. (1977). For Mon R2, the models include some cloud emission outside the cores (diameters ~ 0.1 pc), and the temperature is from NH$_3$ data (Henning et al. 1992).

source	size (pc)	mass (M$_\odot$)	luminosity (10^3 L$_\odot$)	T (K)	n(H$_2$) (cm^{-3})	A$_v$ (mag)
Mon R2						
IRS2	0.7	40	7	$\sim$50	1×10^5	50
IRS3	0.7	30	13	$\sim$50	1×10^5	70
DR21	0.65	5700	150	47	2×10^5	$\gg$100
	0.35	2200	150	47	1×10^6	$\gg$100
W3						
IRS4	0.15	200	97	62	3×10^5	280
IRS5	0.15	80	130	68	1×10^5	280

modulation of the signal was used to deduce the Stokes parameters Q and U, and hence p and θ. Integration times ranged from 8 to 20 waveplate cycles each of 5 minutes duration. The data were analysed using a least-squares fit in the SIT reduction package (Nartallo 1995). Despiking was used to improve the fits, and a Kolmogorov-Smirnov test (e.g. Press et al. 1988) was used to eliminate fits with discontinuous Q or U, usually caused by changes in sky transmission. Approximately 7% of the data were rejected in the K-S test.

Instrumental polarization (IP) was measured using Saturn (assumed unpolarized), and was subtracted in the data reduction. The IP level was 1.61 ± 0.03% at 1100 μm, and 0.28 ± 0.04% at 800 μm. The large change in IP percentage as a function of wavelength is due to the effects of the JCMT wind-blind, which has a polarization minimum at around 800 μm.

The sources observed are listed in Table 1. Central positions were Mon R2-IRS2: RA(1950) = 06h 05m 19.4s, Dec.(1950) = –06° 22′ 27″, Mon R2-IRS3: 06h 05m 21.5s, –06° 22′ 29″ (Aspin & Walther 1990), DR21: 20h 37m 14.5s, +42° 09′ 00″ (Minchin & Murray 1994), and W3-IRS4: 02h 21m 43.5s, +61° 52′ 49″ (Oldham et al. 1994). For W3-IRS4 and the point offset to the north, the data were combined with approximately 1 hour of observations made in 1991, which slightly improved the signal-to-noise.

3. Results

The polarization results for the three sources are listed in Table 1, and the deduced magnetic field structures are discussed briefly here. The standard assumption is used, that the grains are magnetically aligned with the net field perpendicular to the observed polarization angle (but see also Sect. 5.1 below). Some

information about the physical properties of the sources is also given, for context (Table 2).

The Mon R2 cloud core, centred near the IRS1 source, has been mapped in 800 μm polarization by Greaves et al. (1995). Our new data for IRS2 and IRS3 support their model. The field directions converge near the dust peak (see Fig. 1 in Greaves et al. 1995), consistent with field lines pulled in during core contraction. There is a significant difference in the θ values at 800 and 1100 μm for IRS3 which is difficult to explain under the normal assumptions (optically thin dust emission in the submillimetre, so the polarization at each wavelength traces exactly the same aligned grains). The origin of position angle variations is discussed further below.

DR21 has been mapped in 800 μm polarization by Minchin & Murray (1994), and the field across the cloud core was found to be quite linear. The new p and θ values show consistency between the two datasets. The mean field orientation is 116°, which is intermediate between that of the core major axis ($\approx 170°$) and the dominant outflow axis ($\approx 70°$). There is as yet no detailed picture for the magnetic field in DR21, but a model for sources with no obvious field alignments has been presented by Minchin et al. (1996).

The W3 cloud has been mapped in 100 and 800 μm polarimetry by Hildebrand et al. (1995) and Greaves et al. (1994). The 800 μm data suggest an hourglass-shaped field centred on IRS5, and the larger-scale 100 μm map indicates that the hourglass field axis lies roughly SE-NW. Near IRS4 (located about 1′ west of IRS5), there appears to be another local distortion in the field, but with a wave-like shape (Fig. 1). The field twists through a right angle at a position between IRS4 and the dust core IRS4S, 20″ to the south (Oldham et al. 1994). Zeeman data show a changing gradient in the line-of-sight field strength near IRS4 (Roberts et al. 1993, their Fig. 4a), which also supports the idea of a distortion in the field.
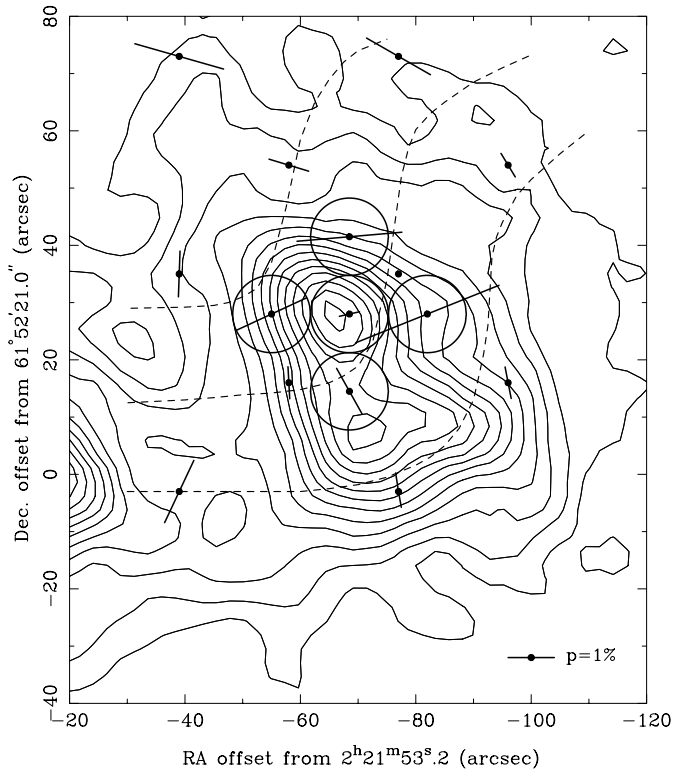
Fig. 1. 800 μm continuum map of W3-IRS4 (from Oldham et al. 1994), with polarization vectors superimposed. The vector length and direction indicate the percentage polarization (see scale) and position angle. Data at 800 μm (this work) are shown within circles representing the 14″ beam size, and 100 μm data (Hildebrand et al. 1995) are shown without circles (beam size of 35″). A suggested field morphology is also shown (dashed lines). IRS4 is located at the centre of the middle circle.

In W3, both the IRS4 and IRS5 sources have a polarization minimum of p(800) $\approx$ 0.5%, compared to surrounding positions with p(800) $\approx$ 1–3% (Greaves et al. 1994, and this paper). This effect is consistent with complex field structure at the star-formation sites, resulting in polarization directions that cancel out within the beam (Minchin & Murray 1994). Core formation has strongly affected the field around both IRS5 and IRS4/IRS4S, but the overall field geometries are seen to differ, even though the cores are physically similar (Table 2). This suggests that the fields are affected by the larger-scale environment, such as cloud internal motions or the presence of HII regions adjacent to IRS5 (Oldham et al. 1994).

4. Comparison with polarization models

4.1. PTEAR mechanism

It has been pointed out by Onaka (1995) that dust grains illuminated anisotropically will have different temperatures depending on the cross-section they present to the radiation source. This can produce a net polarization *without* grain alignment, because the grains oriented with a large surface area towards the source

will be hotter, and thus emit more. This mechanism of polarized thermal emission by anisotropic radiation (PTEAR) can also modify the polarization characteristics when grains are aligned (Onaka 1996). The effects are predicted to be more significant at shorter wavelengths than in the submillimetre.

Our 800 μm observations of W3-IRS5 (Greaves et al. 1994) showed a four-point centro-symmetric polarization pattern that could be explained by PTEAR, with IRS5 as the illuminating source. To test this hypothesis, we have made another four-point polarization map around the IRS4 source in W3, which is very similar to the IRS5 core in luminosity and extinction (Oldham et al. 1994). Thus if PTEAR is a significant effect, IRS4 should also show a centro-symmetric polarization pattern.

As shown in Fig. 1, the polarization vectors around IRS4 are not centro-symmetric. Three of the four offset points have vectors pointing roughly *towards* IRS4, and only the northern point has a centro-symmetric orientation. By considering the Stokes parameter Q (= p cos2θ) expected in PTEAR, we can constrain the magnitude of the effect. For the north and south points, Q should be negative, while for the east and west points, Q should be positive (and the parameter U = p sin2θ should be zero at all positions). In fact, Q has the wrong sign at three of the four points, so another effect, presumably magnetic alignment, must provide a larger Q component of opposite sign.

Further, we can compare the IRS4 results with the Q and U observed for the four points at the same offsets around IRS5 (Greaves et al. 1994). If we assume that *all* the polarization there is due to PTEAR, and exactly the same effects are produced around IRS4, then p(PTEAR) = |Q(IRS5)| and p(magnetic) = $\sqrt{[(Q(IRS4) - Q(IRS5))^2 + U(IRS4)^2]}$. Then the average p(PTEAR) and p(magnetic) are 2.4% and 3.4% respectively, giving p(PTEAR)/p(magnetic) $\approx$ 0.7. If our initial assumption that p(IRS5) $\equiv$ p(PTEAR) is invalid, then this ratio will be an upper limit. These results indicate that magnetic alignment dominates over PTEAR in the submillimetre, even for cores with very luminous sources (L(IRS4) = 10^5 L$_\odot$, Oldham et al. 1994).

4.2. Suprathermal rotation

It was originally suggested by Purcell (1979) that grains could be spun up to suprathermal speeds, when H$_2$ molecules were ejected after forming on the grain surface. This spin-up enhances alignment because the grains are less disoriented by gas-grain collisions. However, free H atoms are needed to adsorb onto the grain surfaces, whereas in molecular clouds nearly all of the hydrogen is in the form of H$_2$. Recently, Sorrell (1995a,b) has proposed a modified model, in which cosmic rays strike grain mantles, ejecting accreted H$_2$ molecules from the surface and providing the necessary torque for spin-up. Lazarian & Roberge (1997) have argued that this torque will not be significant for typical cosmic ray fluxes.

A key prediction of the Sorrell model is that the efficiency depends on the mantle composition. In particular, H$_2$ molecules evaporate rapidly on pure CO mantles, faster than the timescale for a cosmic ray to arrive, so these grains will not spin up,
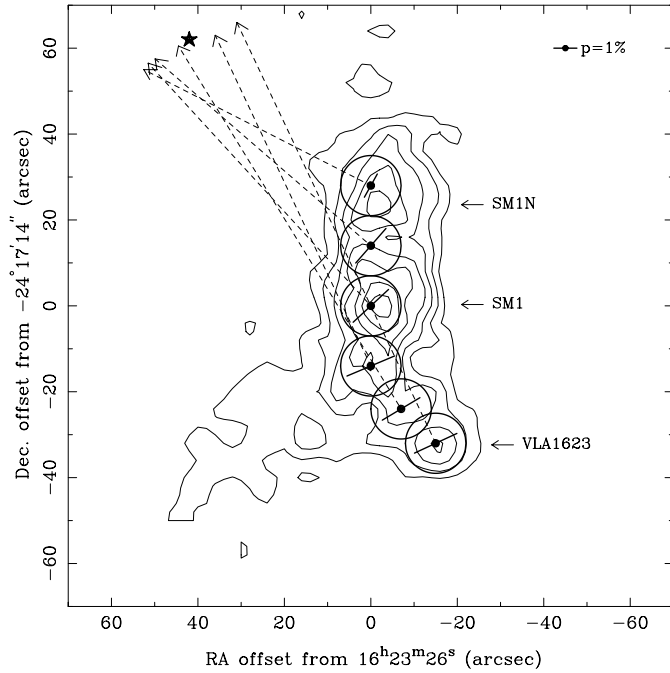
Fig. 2. 800 μm polarization data and dust emission map of ρ Oph A, from Holland et al. (1996). Perpendiculars to the polarization vectors are shown (dotted lines), and they converge near the T Tauri source VSSG27 (star symbol).

whereas grains with H_2O or CO_2 mantles will. Thus p should be much less where CO mantles dominate over H_2O/CO_2 mantles.

We have tested this model using the observations towards the two sources in Mon R2. The line of sight to IRS2 has a deep 4.67 μm CO absorption feature which is not seen towards IRS3 (Geballe 1986). Thus, if the grains around IRS2 cannot align, we expect a much lower p than towards IRS3. In fact, we find that at 800 μm, p is very similar in the two sources, and at 1100 μm the values are consistent within the errors. Further, for IRS2 p(800) is detected at the 95% confidence level (method of Clarke & Stewart 1986), inconsistent with the hypothesis that this source is unpolarized. Thus, at the moderate confidence levels of our data, it appears that CO-mantled grains are aligned in Mon R2, and the model predictions are not supported. A related result is polarization of the 4.67 μm CO ice feature towards W33A (Chrysostomou et al. 1996), which also shows alignment of CO-mantled grains.

4.3. Radiative alignment

Irradiation can affect grain alignment, as molecules may desorb from the grain surface, affecting the spin rate (Lazarian 1995). Also, irradiation of asymmetric grains can cause suprathermal spin-up, and anisotropic radiation fields can provide torques that directly align grains (Draine & Weingartner 1996, 1997).

In Fig. 2, we present a possible example of radiative alignment. The data shown are 800 μm polarization observations of

the SM1/VLA1623 core in ρ Oph A (Holland et al. 1996). It is noteworthy that the perpendiculars to the six observed polarization vectors point near the star VSSG27. The perpendiculars are within $8°$ of the star's direction, on average (with a mean error in the θ values of $12°$), so the convergence on VSSG27 is significant.

This convergence is unlikely to be a chance effect, since there are only a few stars associated with the cloud that could produce aligning radiation. From the K-band survey of Strom et al. (1995), we find only three stars that are (a) bright at 2.2 μm (K-magnitude $\leq$ 12), (b) located to the east of the ridge where the lines converge, and (c) within a projected distance similar to VSSG27. This star is $74''$ from the (0,0) position of the dust ridge, and there are only two other stars within $150''$ which fit our criteria, neither of which is near the convergence point. VSSG27 is a Class II classical T Tauri (André & Montmerle 1994); it is not the most luminous object in the region (Strom et al. 1995), but is an embedded source and therefore likely to be closely associated with the molecular cloud core. These results for ρ Oph suggest that stellar radiation could affect grain alignment in star-forming clouds.

4.4. Wavelength dependence of p and θ

It is expected that the degree of polarization in the submillimetre will be independent of wavelength (e.g. Hildebrand 1988), since the dust emission is usually optically thin, and thus p depends only on alignment efficiency and field morphology. Previous polarimetry observations have suggested p may sometimes be wavelength-dependent, but often such individual cases can be explained by differences in resolution, where a region of complicated magnetic field is observed.

To determine if p can intrinsically depend on wavelength, we have observed a region where the field is very close to linear, the DR21 cloud core (Minchin & Murray 1994). Observations were made at two wavelengths towards three points, using matched beam sizes of $19''$ at both wavelengths. Any variation in p(λ) can thus not be attributed to field structure within the beam. The results (Table 1) show that p does differ with wavelength. For the (0,0) position, p(800) exceeds p(1100) by 0.95 ± 0.34%, where the error is the sum in quadrature of the errors in each of the two measurements. However, for the offset points p(1100) exceeds p(800), by 1.97 ± 0.72% (south) and 0.69 ± 0.58% (north). A wider study of 115–2000 μm polarization in DR21 (Glenn et al. 1997) has shown some additional evidence for wavelength dependence, but the range of beamsizes is large (14–42$''$) which makes the interpretation more complex.

In DR21, the polarization position angles also vary with wavelength by a small amount. The mean value at 800 μm is θ = $25 \pm 3°$ for the three points (our data and Minchin & Murray 1994), while at 1100 μm it is $11 \pm 5°$, significantly lower. These changes in both p and θ suggest that the two wavelengths are *not* equally tracing the same grains, and hence the field structure deduced is somewhat dependent on the choice of wavelength. These results are discussed further below.

5. Discussion

5.1. Grain alignment in molecular clouds

Some general conclusions can be drawn from the above results. Firstly, the PTEAR mechanism has been shown to be less important than grain alignment in producing submillimetre polarization. The W3-IRS4 data indicate p(PTEAR)/p(magnetic) ≤ 0.7, even for a very bright illuminating source. Another possible non-magnetic mechanism is scattering, which produces polarization in the optical/near-IR (e.g. Bastien 1996), but this is unlikely to be effective in the submillimetre, except in unusual sources where many of the grains are millimetre-sized.

Alignment mechanisms are made more effective if the grains are spun up to suprathermal speeds, but the mechanism using cosmic ray absorption is inconsistent with the Mon R2 data. Spin-up via radiative torque on asymmetrical grains is more promising, and the ρ Oph data suggest that radiation may even directly align grains. This would imply that it is *not* the magnetic field alone that determines the net grain orientation, and thus magnetic field maps deduced from the perpendiculars to polarization vectors (such as Fig. 1) could be misleading.

Other proposed grain alignment mechanisms include superparamagnetic and mechanical processes. Superparamagnetism occurs if small clusters of ferromagnetic or ferrimagnetic material exist in the grains (Draine 1996; Mathis 1986), but Roberge (1996) has found that unrealistically large temperature differences are required (e.g. $T_{gas} \sim 5 \times T_{dust}$). In contrast, mechanical alignment is probable in our sources. Grains can be aligned by collisions with gas molecules, if the gas-grain drift speeds are supersonic (Gold 1951; Roberge et al. 1995; Lazarian 1996b). Mon R2, DR21 and W3 all contain extended outflow systems (Tafalla et al. 1997; Garden et al. 1991; Mitchell et al. 1991), where supersonic flow occurs within the clouds. In a related paper we discuss evidence for polarization correlated with gas-grain drift speeds (Greaves & Holland 1999).

We conclude that mechanical and radiative alignment mechanisms are the most consistent with the data, while superparamagnetism, scattering and PTEAR effects are not significant.

5.2. Wavelength dependence and grain populations

We have also used multi-wavelength observations to search for variations in polarization levels. These are unexpected in the submillimetre, because for optically thin sources in the Rayleigh-Jeans part of the blackbody spectrum, the flux density is proportional to $\nu^2 T \tau_0$ (where ν is the frequency, and T and τ_0 are the grain temperature and opacity), and thus the flux density *ratios* are independent of wavelength. Then considering a mixture of two grain types, the net polarization can be expressed as

$$p_{net} = (p_1 S_1 + p_2 S_2)/(S_1 + S_2)$$
$$= (p_1 S_1/S_2 + p_2)/(S_1/S_2 + 1) \qquad (1)$$

(Hildebrand 1988), where S and p are the flux densities and intrinsic polarization levels of the grain populations, numbered 1 and 2. (Note that this expression assumes that all the grains are
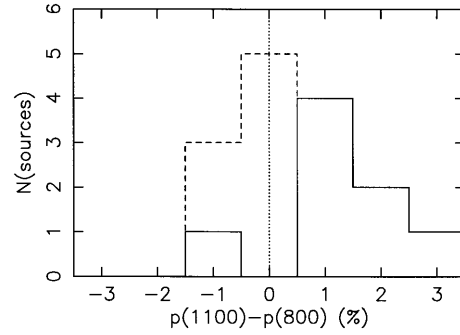

Fig. 3. Distribution of p(1100)–p(800). The dashed portions of the histogram show sources where the polarization difference is less than its error. Data are from this work; Greaves & Holland (1998); Greaves et al. (1997, 1995, 1994); Holland et al. (1996); Minchin et al. (1995); Tamura et al. (1995); Vallée & Bastien (1995); Minchin & Murray (1994); Flett & Murray (1991).

aligned by the same magnetic field, so the **p** vectors can be added linearly.) Then if S_1/S_2 is constant in Eq. (1), p_{net} is constant, and measured values should be the same at all wavelengths.

However, in many sources the grains behave instead as greybodies, i.e. the opacity is frequency-dependent. In this case, the flux density will be proportional to $\nu^{2+\beta} T \tau_0$, where β is the grain opacity index. Then if there are two grain populations with different β indices, S_1/S_2 is *not* constant, and p_{net} can be wavelength dependent. For the two population case, the difference in observed p_{net}, for two wavelengths a and b, can be expressed as

$$\Delta p = (p_1 R_a + p_2)/(R_a + 1) - (p_1 R_b + p_2)/(R_b + 1)$$
$$= \frac{(p_1 - p_2)(R_a - R_b)}{(R_a + 1)(R_b + 1)} \qquad (2)$$

where R is the flux density ratio S_1/S_2. Thus the observed change in polarization with wavelength, Δp, depends on the two intrinsic p values and the two flux density ratios. Alternatively, this can be expressed as a dependence on the difference in beta indices, since $R_a = R_b \times (b/a)^{\beta_1 - \beta_2}$.

The expression above shows that p could be wavelength dependent in any source with mixed grains. To determine whether such effects are common, we have searched for published JCMT polarimetry data on dust sources at wavelengths of 1100 and 800 μm. Fig. 3 shows the distribution of the resulting fifteen values of p(1100)–p(800).

Of these fifteen data points, eight are statistically significant (sources within the solid histogram bars). Of these, seven have p(1100) > p(800), and one source has p(800) > p(1100). Therefore in the majority of cases p *increases* with wavelength, while in most of the remaining sources the p-differences are small or not significant above the error. It could be argued that p(800) and p(1100) differ because of resolution effects, as the beam sizes ranged from $14''$ to $19''$. However, there is no general trend of p(1100)–p(800) with source distance, as would be expected if complex field structure were better resolved in closer sources.

We now compare the observed Δp values for 1100 and 800 μm with the values that can be derived using Eq. (2). The
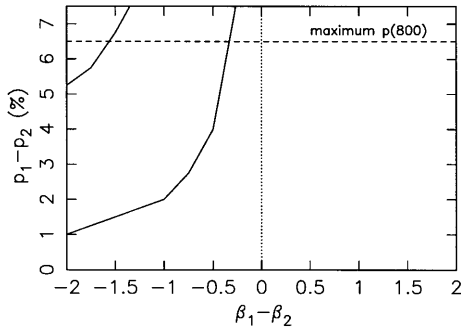
Fig. 4. Plot of the p_1-p_2, $\beta_1-\beta_2$ plane showing the region corresponding to the observed mean p(1100)-p(800) value. For two grain populations with equal flux densities at $800\,\mu m$, this region lies between the solid curved lines, and both bounds are moved upwards for other flux ratios. An upper boundary is indicated by the dashed line at 6.5% polarization, which is the maximum p(800) seen in observations (Minchin & Murray 1994).

range of β values used was 0 to 2, corresponding roughly to the observed range in interstellar clouds. Fig. 4 shows the model results for two grain populations, in a plane of p_1-p_2 versus $\beta_1-\beta_2$. The observed mean p(1100)–p(800) is $0.48 \pm 0.33\%$ (standard error of the fifteen observations), and this value is reproduced in the area within the curved lines. The required grain characteristics are $p_1-p_2 \geq 1\%$ and/or $\beta_1-\beta_2 \leq 0.3$. An additional effect could arise if one of the grain populations is very cold, so that the emission is not in the Rayleigh-Jeans tail and the fluxes are proportional to $B_\nu(T)$, not T. However, even for 10 K grains the required p_1-p_2 differences are large ($\sim 7\%$ for p(1100)–p(800) = 0.48%), so this effect is likely to be less significant.

Fig. 4 shows that the grain population with the larger intrinsic polarization, p_1, must have a smaller opacity index ($\beta_1 < \beta_2$). This is in good agreement with previous studies: elongated grains can have a low value of β (Beckwith & Sargeant 1991), and also be more efficiently aligned (Roberge 1996). However, it should be noted that β indices may also reflect grain size and composition (Beckwith & Sargeant 1991; Mannings & Emerson 1994).

The published JCMT data also show some wavelength dependence in the polarization directions. Of the fifteen sources in Fig. 3, thirteen have position angles determined at both wavelengths, and of these seven have a $\theta(800)-\theta(1100)$ difference that is significant at the 1σ level or more. For all thirteen sources, the mean $\theta(800)-\theta(1100)$ is $17° \pm 4°$ (standard error).

The grain mixture hypothesis is also relevant to variations in θ (although some of the larger differences are best explained by unresolved field structure, e.g. Greaves & Holland 1998). At any particular wavelength the polarization is biased towards the grain population with the highest fraction of the polarized flux. Then if the grain populations are not cospatial, and the field is not uniform along the line of sight, different θ can result at different wavelengths. Since grain properties are expected to vary with position in a cloud (e.g. Goodman 1995), it is likely that grain populations will indeed be non-cospatial. Alternatively,

the grains could be mixed but one population might be aligned radiatively (see Sect. 4.3), and thus θ (and p_{net}) changes would occur at the wavelength where these grains dominate the flux. This hypothesis would suggest larger changes with more illumination, but a counter-example occurs in DR21, where the south point has more marked p,θ variations with wavelength than the centre position. Further modelling is needed to determine the importance of this effect.

Finally, to determine if the grain mixture hypothesis is really applicable to molecular clouds, we have searched the literature for β indices of the sources in Fig. 3. Values were found for twelve of the sources (not the three positions in DR21), and the average β is 1.3 with a 1σ range of ± 0.4. This is reasonably consistent with our requirement for mixed β values, as the overall β value should then be intermediate between 0 and 2.

6. Conclusions

Polarization data at 800 and $1100\,\mu m$ have been obtained for Mon R2, DR21 and W3-IRS4. The results imply that submillimetre polarization is dominated by grain alignment, rather than heating effects; however, source radiation may be important for the spin-up and alignment of grains. The most likely mechanisms of grain alignment are mechanical and possibly radiative processes, while superparamagnetism is unlikely, as the gas-grain temperature differences required are not present in these molecular clouds.

Examination of published data has shown that the polarization percentage and position angle can be wavelength dependent in the submillimetre. The percentage difference is almost always in the sense that p(1100) exceeds p(800), an effect which can be explained by mixtures of grains in the clouds (if less spherical grains are better aligned). The polarization is then biased towards the grain population with the most polarized flux. This can also produce a wavelength bias in the position angle, so the choice of observing wavelength in the submillimetre is not as immaterial as is frequently supposed. In the future, multi-wavelength polarimetry is desirable to give an overall picture of the magnetic field directions, and the effects of radiation on grain alignment should also be further investigated. The new Submillimetre Common-User Bolometer Array (SCUBA; Holland et al. 1999) has a multi-wavelength polarimetry mode that is now being commissioned at the JCMT, which should shortly be able to address these questions.

References

André P., Montmerle T., 1994, ApJ 420, 837
Aspin C., Walther D.M., 1990, A&A 235, 387
Bastien P., 1996, In: Roberge W.G., Whittet D.C.B. (eds.) Polarimetry of the Interstellar Medium. ASP Conference Series Vol. 97, 297
Beckwith S.V.W., Sargeant A.I., 1991, ApJ 381, 250

Chrysostomou A., Hough J.H., Whittet D.C.B., et al., 1996, ApJ 465, L61

Clarke D., Stewart B.G., 1986, Vistas in Astronomy 29, 27

Davis L., Greenstein J.L., 1951, ApJ 114, 206

Draine B.T., 1996, In: Roberge W.G., Whittet D.C.B. (eds.) Polarimetry of the Interstellar Medium. ASP Conference Series Vol. 97, 16

Draine B.T., Weingartner J.C., 1996, ApJ 470, 551

Draine B.T., Weingartner J.C., 1997, ApJ 480, 633

Duncan W.D., Robson E.I., Ade P.A.R., Griffin M.J., Sandell G., 1990, MNRAS 243, 126

Flett A.M., Murray A.G., 1991, MNRAS 249, 4P

Garden R.P., Geballe T.R., Gatley I., Nadeau D., 1991, ApJ 366, 474

Geballe T.R., 1986, A&A 162, 248

Glenn J., Walker C.K., Jewell P.R., 1997, ApJ 479, 325

Gold T., 1951, Nat 169, 322

Goodman A.A., 1995, In: Haas M.R., Davidson J.A., Erickson E.F. (eds.) Airborne Astronomy Symposium on the Galactic Ecosystem: From Gas to Stars to Dust. ASP Conference Series Vol. 73, 45

Greaves J.S., Holland W.S., 1998, A&A 333, L23

Greaves J.S., Holland W.S., 1999, MNRAS 302, L45

Greaves J.S., Murray A.G., Holland W.S., 1994, A&A 284, L19

Greaves J.S., Holland W.S., Murray A.G., 1995, A&A 297, L49

Greaves J.S., Holland W.S. Ward-Thompson D., 1997, ApJ 480, 255

Harvey P.M., Campbell M.F., Hoffman W.F., 1977, ApJ 211, 786

Henning Th., Chini R., Pfau W., 1992, A&A 263, 285

Hildebrand R.H., 1988, QJRAS 29, 327

Hildebrand R.H., 1996, In: Roberge W.G., Whittet D.C.B. (eds.) Polarimetry of the Interstellar Medium. ASP Conference Series Vol. 97, 254

Hildebrand R.H., Dragovan M., 1997, ApJ 450, 663

Hildebrand R.H., Dotson J.L., Dowell C.D., et al., 1995, In: Haas M.R., Davidson J.A., Erickson E.F. (eds.) Airborne Astronomy Symposium on the Galactic Ecosystem: From Gas to Stars to Dust. ASP Conference Series Vol. 73, 97

Holland W.S., Robson E.I., Gear W.K., et al., 1999, MNRAS (in press)

Holland W.S., Greaves J.S., Ward-Thompson D., André P., 1996, A&A 309, 267

Lazarian A., 1995, MNRAS 277, 1235

Lazarian A., 1996a, In: Roberge W.G., Whittet D.C.B. (eds.) Polarimetry of the Interstellar Medium. ASP Conference Series Vol. 97, 438

Lazarian A., 1996b, In: Roberge W.G., Whittet D.C.B. (eds.) Polarimetry of the Interstellar Medium. ASP Conference Series Vol. 97, 433

Lazarian A., Roberge W.G., 1997, MNRAS 287, 941

Mannings V., Emerson J.P., 1994, MNRAS 267, 361

Mathis J.S., 1986, ApJ 308, 281

Minchin N.R., Murray A.G., 1994, A&A 286, 579

Minchin N.R., Sandell G., Murray A.G., 1995, A&A 293, L61

Minchin N.R., Bonifacio V.H.R., Murray A.G., 1996, A&A 315, L5

Mitchell G.F., Maillard J.-P., Hasegawa T.I., 1991, ApJ 371, 342

Murray A.G., 1991, Ph.D. Thesis, University of Aberdeen

Murray A.G., Flett A.M., Murray G., Ade P.A.R., 1992, Infrared Phys. 33, 113

Nartallo R., 1995, Ph.D. Thesis, University of Edinburgh

Oldham P.G., Griffin M.J., Richardson K.J., Sandell G., 1994, A&A 284, 559

Onaka T., 1995, ApJ 439, L21

Onaka T., 1996, In: Roberge W.G., Whittet D.C.B. (eds.) Polarimetry of the Interstellar Medium. ASP Conference Series Vol. 97, 72

Press W.H., Flannery B.P., Teukolsky S.A., Vetterling W.T., 1988, In: Numerical Receipes in C. Cambridge University Press, 487

Purcell E.M., 1979, ApJ 231, 404

Richardson K.J., White G.J., Phillips J.P., Avery L.W., 1986, MNRAS 219, 167

Roberge W.G., 1996, In: Roberge W.G., Whittet D.C.B. (eds.) Polarimetry of the Interstellar Medium. ASP Conference Series Vol. 97, 401

Roberge W.G., Hanany S., Messinger D.W., 1995, ApJ 453, 238

Roberts D.A., Crutcher R.M., Troland T.H., Goss W.M., 1993, ApJ 412, 675

Sorrell W.H., 1994, MNRAS 268, 40

Sorrell W.H., 1995a, MNRAS 273, 169

Sorrell W.H., 1995b, MNRAS 273, 187

Strom K.M., Kepner J., Strom S.E., 1995, ApJ 438, 813

Tafalla M., Bachiller R., Wright M.C.H., Welch W.J., 1997, ApJ 474, 329

Tamura M., Hough J.H., Hayashi S.S., 1995, ApJ 448, 346

Vallée J.P., Bastien P., 1995, A&A 294, 831

Wardle J.F.C., Kronberg P.P., 1974, ApJ 194, 249